272 W quasi-single-mode picosecond pulse laser of ytterbium-doped large-mode-area photonic crystal fiber

Meng Wang (王 孟)[1,2], Fan Wang (王 璠)[1,2], Suya Feng (冯素雅)[1,*], Chunlei Yu (于春雷)[1,], Shikai Wang (王世凯)[1], Qinling Zhou (周秦岭)[1], Lei Zhang (张 磊)[1], Fengguang Lou (楼风光)[1], Danping Chen (陈丹平)[1], and Lili Hu (胡丽丽)[1,***]**

[1]*Key Laboratory of Materials for High Power Laser, Shanghai Institute of Optics and Fine Mechanics, Chinese Academy of Sciences, Shanghai 201800, China*

[2]*University of Chinese Academy of Sciences, Beijing 100049, China*

**Corresponding author: fsy@siom.ac.cn; **corresponding author: sdycllcy@163.com; ***corresponding author: hulili@siom.ac.cn*

Received January 26, 2019; accepted March 22, 2019; posted online June 17, 2019

A large-mode-area (LMA) ytterbium-doped photonic crystal fiber (PCF) with core NA of 0.034 and core diameter of 50 μm was made by the stack-and-draw technique. The core is formed by $Yb^{3+}/Al^{3+}/F^{-}/P^{5+}$ co-doped silica glass containing 0.09 mol% Yb_2O_3 with an absorption coefficient at 976 nm up to 3.2 dB/m. The core glass with homogeneous distribution of Yb^{3+} ions and refractive index difference of 4×10^{-4} compared with pure silica was prepared by the sol-gel method and heat homogenization at 2000°C. Laser power amplification of this LMA PCF was studied using a seed source of 21 ps pulse duration and 48.7 MHz repetition rate at 1030 nm wavelength. With pump power of 520 W, a maximum 272 W (266 kW peak power) quasi-single-mode laser output with M^2 of 2.2 was achieved in a 4.7 m fiber length bent at a diameter of 47 cm with slope efficiency of 52%, and no obvious mode instability, stimulated Raman scattering, or thermal damage on the end facet of the fiber were observed.

OCIS codes: 140.3538, 140.3615, 140.3510, 160.5690.
doi: 10.3788/COL201917.071401.

Yb^{3+}-doped silica fibers have attracted extensive studies for their application in high-power lasers and become ubiquitous in scientific and industrial applications[1–4]. With the increasing of laser output power, the traditional double-cladding fibers suffer nonlinear effects and even damage of the end facet of fibers[5,6]. An effective approach to solve these problems is to increase the effective area (A_{eff}) of the fundamental mode, which is defined as the large-mode-area (LMA) fiber[7,8]. LMA fibers can effectively reduce laser power density, thereby increasing the thresholds of thermal damage and suppressing nonlinear effects during high-power pumping. Therefore, Yb^{3+}-doped LMA fibers have been the subject of intense research during the past decade[9–12].

LMA fibers can effectively inhibit nonlinear effects, but their laser beam quality could seriously deteriorate with the increase of the core diameter[13]. For an effective single-mode operation, researchers around the world have devoted considerable effort to optimizing the design of LMA fibers for robust single modeness[14]. Several types of LMA fibers are currently proposed, such as large-pitch fibers (LPFs)[15], all-solid photonic bandgap fibers (AS-PBFs)[16], all-solid single trench fibers[17], and polygonal chirally coupled core (P-CCC) fibers[18]. Many LMA fiber designs require the refractive indices of the fiber core and cladding to be nearly equal. It is noted that the greatest challenge in fabricating active LMA fibers is the preparation of the Yb-doped preform, requiring the lowering of the refractive index of high-level Yb^{3+}-doped silica core glasses whilst maintaining high optical homogeneity. At present, the commercial preparation technique, modified chemical vapor deposition (MCVD), with solution doping makes it difficult to obtain the large size of an active core of an ideally uniform refractive index profile. An alternative technique is to utilize gas-phase doping in the MCVD system, where a large-size Yb^{3+}-doped silica core with high homogeneity could be achieved[19], but the refractive index difference between core and cladding should be further reduced. Meanwhile, scientists have begun to explore non-chemical vapor deposition (CVD) methods to prepare core glass rods for rare-earth-doped LMA fibers, such as direct nanoparticle deposition (DND)[20], reactive powder sintering of silica (REPUSIL)[21,22], and sol-gel methods[23]. Hamzaoui *et al.*[24] have reported that F/Yb co-doped silica glasses were prepared by a low-temperature sol-gel method and obtained a maximum output power of 133 mW and slope efficiency of 70.4% from the photonic crystal fiber (PCF). In recent years, our groups have been committed to the preparation of large Yb^{3+}-doped silica glass rods with low refractive index and high homogeneity by the modified sol-gel method combined with high-temperature sintering. In our previous studies, Wang *et al.*[25] reported a 255 W picosecond master oscillator power amplifier (MOPA) laser based on self-made Yb-doped very-LMA PCFs, while, due to the relatively high refractive index, the beam quality of the laser was not ideal. Wang *et al.*[26] reported a uniform $Yb^{3+}/Al^{3+}/F^{-}/P^{5+}$ with 0.075 mol% Yb_2O_3 co-doped silica-core glass and prepared

 © 2019 Chinese Optics Letters

an LMA PCF with 50 μm core diameter, from which an average amplified power of 97 W and light–light efficiency of 54% were achieved. However, further improvement of output power was limited by the nonlinear behaviors of the PCF because of the relatively low doping content of Y_2O_3, leading to a longer PCF for test.

In this Letter, based on our previous work of a $Yb^{3+}/Al^{3+}/F^{-}/P^{5+}$ co-doped silica rod fabricated by the sol-gel method, the glass rod with high content of Yb_2O_3 doping was prepared to reduce the active LMA PCF length as the amplifier and the nonlinear effect. In order to improve the homogeneity of Yb^{3+} ion doping, the core glass was homogenized with the help of an MCVD lathe. A high-Yb-doping LMA PCF was fabricated, and its amplified laser performances were studied.

A $Yb^{3+}/Al^{3+}/F^{-}/P^{5+}$ co-doped silica rod was prepared by the sol-gel method, which has been described exhaustively in our previous studies[10,26]. The molar composition of the rod (named the initial rod) was $0.09Yb_2O_3 - 0.9Al_2O_3 - 0.2P_2O_5 - 98.89SiO_2$, and F^{-} with the mean F^{-}/Si^{4+} mass ratio of 3.0% was introduced in addition. Then, the initial rod was purified and homogenized by the flame at 2000°C in an MCVD lathe to form a core glass rod (named the final rod) with the size of ∅5 mm × 200 mm.

To study the effect of Yb^{3+}-doped rod homogenization by high-temperature flame heating, the relative refractive indices of the initial and final rods were measured with a Photon Kinetics PK 2600 instrument at 633 nm. Figure 1 shows the relative refractive indices profiles of the initial and final rods at the Z50 and Z150 positions (50 mm and 150 mm away from the bottom end of the final rod). It is noteworthy that the obvious fluctuation in the center of the rods is a numerical artifact probably caused by the profile calculation algorithm[27].

In Fig. 1, compared with the initial rod, the refractive index uniformity in the axial and radial directions of the final rod is greatly improved by the high-temperature flame heating. The average refractive index difference of

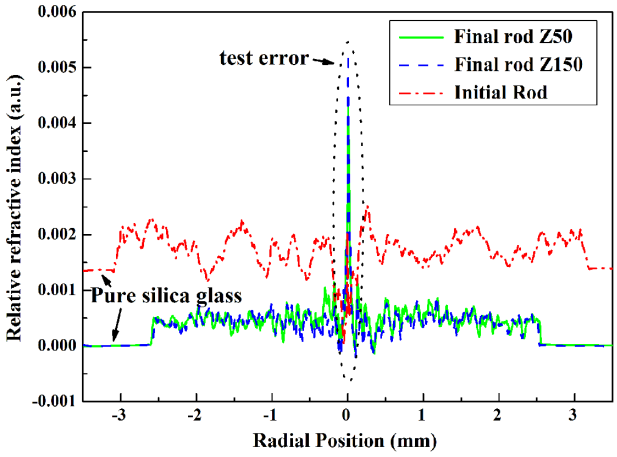

Fig. 1. Relative refractive indices of the initial and homogenized final rods.

the initial rod with respect to pure silica glass (Δn) is about 4×10^{-4} with obvious variation. After purification and thermal homogenization, the fluctuation in the radial direction is about 2×10^{-4}, and in the axial direction, it is very small. The average values of Δn at Z50 and Z150 positions (50 mm and 150 mm away from the bottom end of the final rod) are both about 4×10^{-4}, corresponding to a core NA of 0.034. In the original process, limited by the equipment, the powder made by the sol-gel method was sintered at 1750°C to form glass, which is a relatively low melting temperature for silica glass. This results in the inhomogeneity of the glass. Heated by the high-temperature flame again, the inhomogeneous region was melted thoroughly. Therefore, the uniformity of the rod can be improved significantly.

According to the delocalization effect (characterized by the overlap factor)[28], the preform of the PCF with the final rod was designed and prepared by the stack-and-draw technique. Then, the LMA PCF was drawn at 2000°C under controlled pressure. The micrograph of the PCF cross section is illustrated in Fig. 2(a). The diameters of the Yb^{3+}-doped core, pump cladding, and outer cladding of the PCF are about 50, 260, and 450 μm, respectively. The diameter of the air holes is about 2 μm, and the pitch is about 16 μm. The NA of pump cladding exceeds 0.55, allowing for an efficient launch of the multimode pump laser into the PCF, which is up to 90%.

Figure 3(b) shows the distribution of all components, including Al^{3+}, P^{5+}, Yb^{3+}, and F^{-}, in the PCF core, which was measured by electron probe micro-analyzer mapping analysis (EPMA, JEOL, JXA-8230). It can be observed that the doping Al^{3+}, P^{5+}, Yb^{3+}, and F^{-} ions are distributed randomly and uniformly in the core without any aggregation, further approving the effect of the Yb^{3+}-doped rod homogenized by high-temperature flame heating. From the results, it can be found that the doping concentration of Yb^{3+} ions is about 0.45 wt%. Based on the relatively high content of the Yb^{3+} ion, the absorption coefficient of the PCF at the pump wavelength (976 nm) is about 3.2 dB/m, which was measured by a cut-back method. A 4.7 m length of the PCF was used to characterize the amplification performance in the pulse laser system.

Figure 3 schematically illustrates the MOPA experimental setup. A seed source at 1030 nm wavelength (21 ps pulse duration and 48.7 MHz repetition rate) and a 976 nm laser diode (LD) pump were used in this amplifier setup. The beam quality profile was measured by a high-power laser quality monitor (HP-LQM, Prime).

To investigate the amplification of the PCF under bend, the average output power as a function of launched pump power was measured for different bend diameters from 36 to 47 cm, as shown in Fig. 4(a). The maximum output powers for the bend diameters of 3, 40, 43, and 47 cm are 107, 108, 112, and 120 W, respectively. The corresponding slope efficiencies are about 49%, 50%, 52%, and 55%. It can be found that there is an increasing of the output power and slope efficiency when the bend

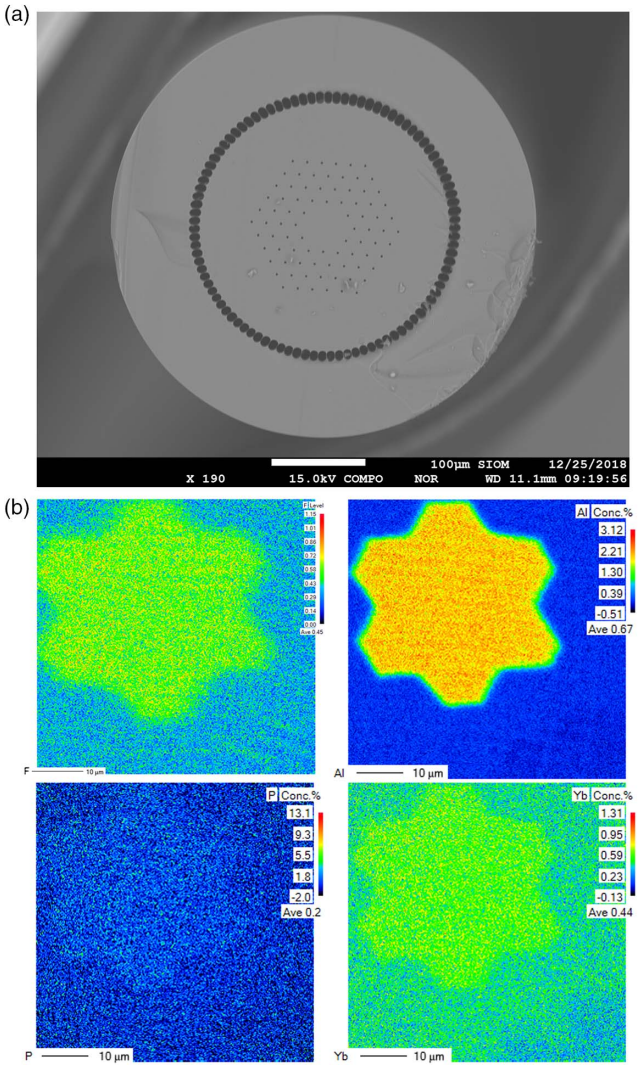

Fig. 2. (a) Microscope image of the fabricated PCF. (b) EPMA mapping analysis of the F^{-}, Al^{3+}, P^{5+}, and Yb^{3+} distribution in the core of the PCF.

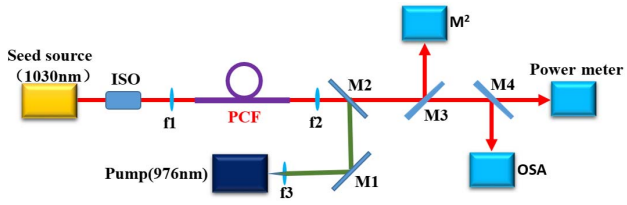

Fig. 3. Experimental setup of a MOPA system.

diameter of the PCF changed from 36 to 47 cm. Moreover, the output power for the bend diameter over 47 cm was measured, and the power did not obviously increase. Compared with other low NA double-cladding fibers[29], this PCF shows a stronger bending resistance. Choosing a 47 cm bend diameter, the amplified laser performances were investigated by launched 520 W pump power into the PCF. Figure 4(b) presents the amplified output power versus launched pump power. Corresponding to the pulse

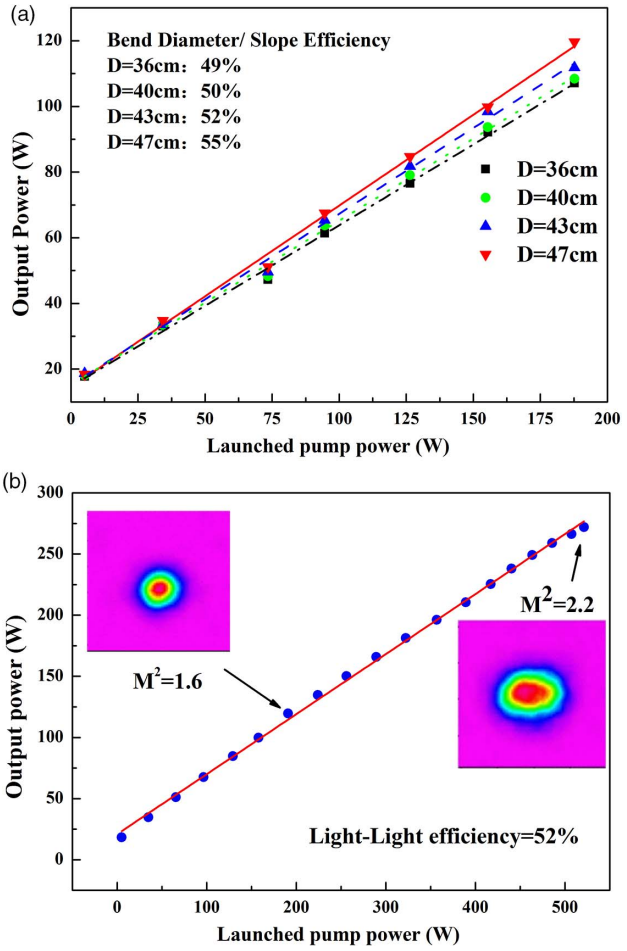

Fig. 4. (a) Amplified output power versus launched pump power at different bend diameters. (b) Average output power versus launched pump power at 47 cm bend diameter. Inset: laser beam profiles at 120 and 272 W output power.

energy of 5.6 μJ and peak power of 266 kW, 272 W output power of the amplified laser was achieved, and the light–light efficiency is calculated to be 52%. The insets of Fig. 4(b) show the laser beam profiles in the far field at 120 and 272 W output powers. The M^2 (beam quality factor) of the amplified laser with 120 W power is about 1.6. The M^2 increases to 2.2 when the output power is up to 272 W. This can be related to the thermal effect due to the increasing pump power in the fiber, where the refractive index difference between the Yb^{3+}-doped core and silica cladding was slightly raised, which resulted in the mismatch of the refractive index between core and cladding[30].

Figure 5(a) shows the temporal stability of 120 W output power for 2 h. During 2 h, the power stability is better than 1.1% RMS (root mean square). No obvious laser output power decaying was observed in the test period. Figure 5(b) depicts the typical output laser spectrum under irradiation of 520 W pump power, and the inset shows the pulse profile of the seed. The pulse width is about 21 ps when obtaining 272 W output power. The optical signal-to-noise ratio (OSNR) is larger than 30 dB, and the spectral bandwidth

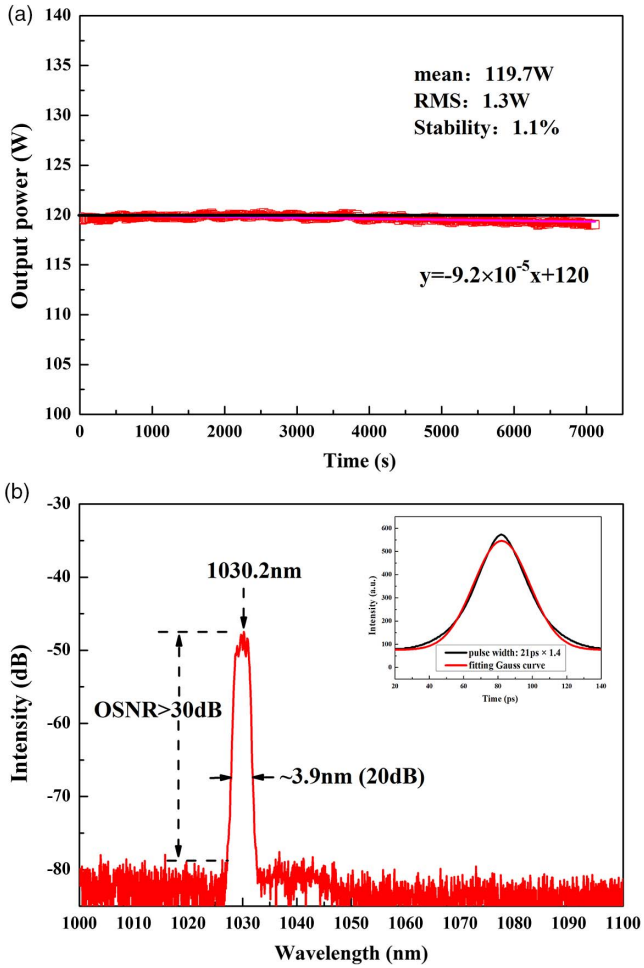

Fig. 5. (a) Output power as a function of time. (b) Output laser spectrum with launched pump power of 520 W. Inset: pulse profile of the seed.

at 20 dB is about 3.9 nm, which is similar to the seed. The self-phase modulation pumped at 520 W is not obviously observed. The center wavelength of the laser peak is about 1030.2 nm. From the spectrum, no stimulated Raman scattering (SRS) was observed. With launched 520 W pumping power, the mode instability did not appear, and the thermal damage did not happen on the end facet of the PCF. However, when the pumping power exceeded 520 W, the mode instability could be observed, and it became more and more serious with the increase of pumping power. Therefore, this PCF with Yb^{3+}-doped core glass fabricated by the sol-gel method and homogenized by high-temperature flame heating presents satisfactory amplified laser performances. To the best of our knowledge, our active LMA PCF exhibits the best performance in terms of beam quality and maximum laser output power in the direct picosecond amplified system.

In this work, the PCF core rod containing 0.09 mol% Yb_2O_3 and co-doping $Al^{3+}/F^{-}/P^{5+}$ ions was fabricated by the sol-gel method and homogenized by the high-temperature flame with an MCVD lathe. The refractive index uniformity of core glass in both the axial and radial directions was greatly improved. Using this core glass, a 50 μm core diameter LMA PCF was fabricated. The LMA PCF amplifier successfully achieved 120 W average power with M^2 of 1.6 using a 4.7 m length under 47 cm diameter bending. No obvious laser output power decaying was observed for about 2 h. The maximum average amplified power of 272 W and slope efficiency of 52% were obtained at pumping power of 520 W, with the OSNR larger than 30 dB and the FWHM about 3.7 nm. No mode instability and SRS effect or thermal damage threshold on the end face of the PCF could be observed at the maximum pump power. We demonstrate that the active LMA PCF prepared by the sol-gel method and thermal homogenization is a promising gain medium for ultrafast and high-power amplified laser systems.

This work was financially supported by the National High Technology Research and Development Program of China (No. 2016YFB0402201).

References

1. D. J. Richardson, J. Nillsson, and W. A. Clarkson, J. Opt. Soc. Am. B **27**, B63 (2010).
2. M. Leich, W. He, S. Grimm, J. Kobelke, Y. Zhu, B. Müller, J. Bierlich, H. Bartelt, and M. Jäger, Proc. SPIE **9344**, 93440T (2015).
3. M. A. Abdelalim, H. E. Kotb, H. Anis, and S. Tchouragoulov, Photon. Res. **4**, 277 (2016).
4. H. Yu, X. Wang, H. Zhang, R. Su, P. Zhou, and J. Chen, J. Lightwave Technol. **34**, 4271 (2016).
5. E. Coscelli, F. Poli, T. T. Alkeskjold, M. M. Jorgensen, L. Leick, J. Broeng, A. Cucinotta, and S. Selleri, J. Lightwave Technol. **30**, 3494 (2012).
6. C. Jauregui, J. Limpert, and A. Tünnermann, Nat. Photon. **7**, 861 (2013).
7. J. Limpert, T. Schreiber, S. Nolte, H. Zellmer, T. Tünnermann, R. Iliew, F. Lederer, J. Broeng, G. Vienne, A. Petersson, and C. Jakobsen, Opt. Express **11**, 818 (2003).
8. W. He, M. Leich, S. Grimm, J. Kobelke, Y. Zhu, H. Bartelt, and M. Jäger, Laser Phys. Lett. **12**, 015103 (2014).
9. W. Xu, Z. Lin, M. Wang, S. Feng, L. Zhang, Q. Zhou, D. Chen, L. Zhang, S. Wang, C. Yu, and L. Hu, Opt. Lett. **41**, 504 (2016).
10. S. Wang, W. Xu, F. Wang, F. Lou, L. Zhang, Q. Zhou, D. Chen, S. Feng, M. Wang, C. Yu, and L. Hu, Opt. Mater. Express **7**, 2012 (2017).
11. H. Wei, K. Chen, Y. Yang, and J. Li, Opt. Express **24**, 8978 (2016).
12. X. Ge, J. Yu, W. Liu, S. Ruan, C. Guo, Y. Chen, P. Yan, and P. Hua, Chin. Opt. Lett. **16**, 020010 (2018).
13. J. Limpert, A. Liem, M. Reich, T. Schreiber, S. Nolte, H. Zellmer, A. Tünnermann, J. Broeng, A. Petersson, and C. Jakobsen, Opt. Express **12**, 1313 (2004).
14. P. Maji and R. Das, Chin. Opt. Lett. **15**, 070606 (2017).
15. H. Otto, F. Stutzki, N. Modsching, C. Jauregui, J. Limpert, and A. Tünnermann, Opt. Lett. **39**, 6446 (2014).
16. F. Kong, G. Gu, T. W. Hawkins, M. Jones, J. Parsons, M. T. Kalichevsky-Dong, B. Pulford, I. Dajani, and L. Dong, Proc. SPIE **10083**, 1008311 (2017).
17. D. Jain, Y. Jung, M. Nunez-Velazquez, and J. K. Sahu, Opt. Express **22**, 31078 (2014).
18. X. Ma, C. Zhu, I.-N. Hu, A. Kaplan, and A. Galvanauskas, Opt. Express **22**, 9206 (2014).

19. V. Petit, R. P. Tumminelli, J. D. Minelly, and V. Khitrov, Proc. SPIE **9728**, 97282R (2016).
20. J. J. Koponen, L. C. Petit, T. Kokki, V. Aallos, J. Paul, and H. Ihalainen, Opt. Eng. **50**, 111605 (2011).
21. K. Schuster, S. Unger, C. Aichele, F. Lindner, S. Grimm, D. Litzkendorf, J. Kobelke, J. Bierlich, K. Wondraczek, and H. Bartelt, Adv. Opt. Technol. **3**, 447 (2014).
22. V. V. Velmiskin, O. N. Egorova, V. Mishkin, K. Nishchev, and S. L. Semjonov, Proc. SPIE **8426**, 842601 (2012).
23. U. Pedrazza, V. Romano, and W. Lüthy, Opt. Mater. **29**, 905 (2007).
24. H. E. Hamzaoui, G. Bouwmans, A. Cassez, L. Bigot, B. Capoen, M. Bouazaoui, O. Vanvincq, and M. Douay, Opt. Lett. **42**, 1408 (2017).
25. Z. Wang, Q. Li, Z. Wang, F. Zou, Y. Bai, S. Feng, and J. Zhou, Chin. Opt. Lett. **14**, 081401 (2016).
26. F. Wang, L. Hu, W. Xu, M. Wang, S. Feng, J. Ren, L. Zhang, D. Chen, N. Ollier, G. Gao, C. Yu, and S. Wang, Opt. Express **25**, 25960 (2017).
27. A. Langner, G. Schötz, M. Such, T. Kayser, V. Reichelc, S. Grimm, J. Kirchhof, V. Krause, and G. Rehmann, Proc. SPIE **6873**, 687311 (2008).
28. L. Wang, D. He, C. Yu, S. Feng, D. Chen, and L. Hu, IEEE J. Sel. Top. Quantum Electron. **24**, 0900104 (2018).
29. F. Beier, C. Hupel, S. Kuhn, S. Hein, J. Nold, F. Proske, B. Sattler, A. Liem, C. Jauregui, J. Limpert, N. Haarlammert, T. Schreiber, R. Eberhardt, and A. Tünnermann, Opt. Express **25**, 14892 (2017).
30. C. Jauregui, T. Eidam, H. Otto, F. Stutzki, F. Jansen, J. Limpert, and A. Tünnermann, Opt. Express **20**, 12912 (2012).